· Article ·
doi: 10.13679/j.advps.2014.4.00234

Advances in Polar Science
December 2014 Vol. 25 No. 4: 234-245

Arctic sea ice and atmospheric circulation under the abrupt4xCO2 scenario

YU Xiaoyong[1], Annette Rinke[1,2], JI Duoying[1], CUI Xuefeng[1] & John C. Moore[1*]

[1] State Key Laboratory of Earth Surface Processes and Resource Ecology, College of Global Change and Earth System Science, Beijing Normal University, Beijing 100875, China;

[2] Alfred Wegener Institute Helmholtz Centre for Polar and Marine Research, Potsdam, Germany

Received 31 May 2014; accepted 25 November 2014

Abstract We analyze sea ice changes from eight different earth system models that have conducted experiment abrupt4xCO2 of the Coupled Model Intercomparison Project Phase 5 (CMIP5). In response to abrupt quadrupling of CO2 from preindustrial levels, Arctic temperatures dramatically rise by about 10°C—16°C in winter and the seasonal sea ice cycle and sea ice concentration are significantly changed compared with the pre-industrial control simulations (piControl). Changes of Arctic sea ice concentration are spatially correlated with temperature patterns in all seasons and highest in autumn. Changes in sea ice are associated with changes in atmospheric circulation patterns at heights up to the jet stream. While the pattern of sea level pressure changes is generally similar to the surface air temperature change pattern, the wintertime 500 hPa circulation displays a positive Pacific North America (PNA) anomaly under abrupt4xCO2-piControl. This large scale teleconnection may contribute to, or feedback on, the simulated sea ice cover change and is associated with an intensification of the jet stream over East Asia and the north Pacific in winter.

Keywords **Arctic, sea ice, atmospheric circulation, abrupt4xCO2**

Citation: Yu X Y, Rinke A, Ji D Y, et al. Arctic sea ice and atmospheric circulation under the abrupt4xCO2 scenario. Adv Polar Sci, 2014, 25: 234-245, doi:10.13679/j.advps.2014.4.00234

1 Introduction

Arctic annual surface temperature revealed by reanalysis and satellite data experienced more than twice as much warming as the global average in the last 30 years[1]. Possible explanations for the Arctic amplification of temperature rise are, for example, surface albedo feedbacks, changes in atmospheric moisture and clouds, changes in meridional heat and moisture transports in the atmosphere and ocean[2-3]. The Arctic sea ice extent in all months shows significant ongoing decline over the past decades[4-5]. Sea ice thickness has also declined by about 40% largely due to the loss of thicker, older ice cover[4]. Warming during the 21st century is also expected to be greatest in the Arctic. Historical sea ice decline simulated by climate models tends to be under-predicted compared with observations (1953—2011), although the Coupled Model Intercomparison Project Phase 5 (CMIP5) models simulated sea ice trends are more consistent with satellite observations (1979—2011) than CMIP3[6]. During the 21st century the projected sea ice reduction continues in CMIP5 simulations both under Representative Concentration Pathway (RCP) midrange mitigation emission (RCP4.5) and high emission (RCP8.5) scenarios[6-8].

Change of Arctic sea ice impacts the local, and the northern hemispheric climate in general, for example, it is expected to increase the snow fall over Siberia and northern Canada[9-10], and to affect large scale atmospheric circulation and the East Asian monsoon in summer and winter[11-12]. Reduction of sea ice is also expected to change storm tracks, and teleconnection patterns such as the North Atlantic Oscillation[9, 13-14]. In addition, changes of cloud and cyclone activity impact on, and feedbacks with, the Arctic sea ice[15-16].

* Corresponding author (email: john.moore.bnu@gmail.com)

In order to explore the Arctic response, and associated wider atmospheric circulation changes under future possible high CO_2 concentration, it is useful to look at the robust response to a very high and constant CO_2 concentration scenario. In this study, we focus on investigating the response of Arctic surface air temperature, sea ice, atmospheric circulation and cyclone activity to a quadrupled CO_2 level forcing.

2 Analysis Methods

Eight model groups provide sea ice concentration data that we use here (BNU-ESM, CCSM4, EC-EARTH, GISS-E2-R, IPSL-CM5A-LR, MIROC-ESM, MPI-ESM-LR, NorESM1-M; Table 1). Each model ran two CMIP5 experiments: piControl and abrupt4xCO2. Experiment piControl is a preindustrial control run in which climate has reached steady state, while experiment abrupt4xCO2 initiates from this preindustrial control condition and is then forced by an instantaneous quadrupling of CO_2 from preindustrial levels, which are then held fixed[17]. The eight models used in this study are different in resolution, components, and parameterizations. Moore et al.[18] give details of sea ice components in models while Kravitz et al.[19] list atmosphere, ocean, land components. As the sea ice representation in the different models varies in both resolution and physics (Table 1)[20], we discuss results of individual models in addition to ensemble means. We use the average of first 50 year simulation periods of abrupt4xCO2 and the average of longest piControl experiments to calculate anomalies. The first years, and perhaps decades, of abrupt4xCO2 will not reflect slow feedbacks to global temperature change, and this can be an issue e.g. in estimating frequency distribution of extreme warm or cold events[21], but we note that sea ice is a low inertia part of the system that responds very rapidly to forced change[22], and that sea ice is also very variable on annual time scales. Analysis of the first 50 years of abrupt4xCO2 suggests that all the models except GISS-E2-R require more than 10 years of adjustment time, in fact 30 years seems to be needed in general. This fairly long period of adjustment suggests rather longer feedback loops than often assumed for sea ice (e.g., Thorndike[23]; Bitz and Roe[24]). Hence the first 50 year of abrupt4xCO2 simulation periods is long enough to describe differences of temperature, sea ice and other corresponding climate variables from piControl.

Table 1 Sea ice models used in this study

ESM Model	Sea ice model	Resolution	Ice physics	Reference
BNU-ESM	CICE4.1	300 x 200 boxes	Two-level thermodynamic +Elastic Visco Plastic (EVP) rheology	Hunke and Lipscomb[25]
CCSM4	CICE4.0	~1°x1°	As CICE4+dust and black carbon	Holland et al.[26]
EC-EARTH	LIM2	As ocean ~1°x1°	Two-layer thermodynamic +viscous-plastic	Fichefet and Maqueda[27]
GISS-E2-R	Integrated	As atmosphere ~2°x2.5°	Four-layer thermodynamic +viscous-plastic	Schmidt et al.[28]
IPSL-CM5A-LR	NEMO-LIM2	As ocean 96 x 95 boxes	Two-level thermodynamic +viscous-plastic	Dufresne et al.[29]
MIROC-ESM	COCO3.4	As ocean ~1°x1.4°	EVP rheology, two-category ice, leads parameterization,	K-1 Model Developers [30]
MPI-ESM-LR	Integrated	As ocean ~1.5°x1.5°	Zero-level thermodynamic +viscous-plastic	Notz et al.[31]
Nor-ESM1-M	CICE4 extended	As ocean ~1°x1°	As CICE+melt ponds and aerosols	Bentsen et al.[32]

3 Results

3.1 Surface air temperatures

The ensemble mean of seasonal surface air temperature anomalies of abrupt4xCO2-piControl for the 8 models is shown in Figure 1. Of the four seasons, autumn and winter have the largest warming, about 10°C—16°C higher compared with piControl over the Arctic Ocean. Summer has the smallest warming, about 1°C—4°C higher than piControl. The maximum temperature increase occurs over the central Arctic Ocean in autumn, and over the Barents and Kara seas and Chukchi Sea in winter (Figure 1), which is related to the large sea ice reduction there. These are the regions with sea ice in piControl but absent or significantly reduced in abrupt4xCO2.

3.2 Sea ice extent and concentrations

3.2.1 Sea ice extent

The seasonal cycle of sea ice extent under abrupt4xCO2 and piControl is shown in Figure 2. The sea ice extent is obviously reduced for the abrupt4xCO2 compared with piControl in all the months. The largest reduction occurs in summertime (5 out of 8 models show the Arctic Ocean to be ice free, and the Arctic sea ice extent is reduced by about 8 million km^2 in September). Table 2 shows the annual, multi-year and first-year sea ice area change under abrupt4xCO2 compared with piControl. We have followed Zhang and Walsh[33] in treating the annual minimum sea ice area that occurs in September (Figure 2) as a proxy indicator for multi-year ice area, and that first-year ice (or seasonal ice) area is defined as the difference between the annual

maximum sea ice area (occurring in March) and the multi-year sea ice area (September). The ensemble mean first-year sea ice area is increased by 25% while the multi-year sea ice area is decreased by 89%. For the individual models, all of them show multi-year sea ice reduction by more than 80% and 7 out of 8 models show a first-year sea ice increase by more than 20%. The large loss of multi-year ice suggests a thinner and more mobile ice cover in abrupt4xCO2 than under piControl conditions. The ensemble mean annual sea ice area decreased by 48% under abrupt4xCO2. Note that the initial conditions of sea ice have substantial impact of sea ice change under abrupt4xCO2 in the first years or decades. Models with thinner initial sea ice typically show a larger reduction of the sea ice extent in climate change simulations because the thin ice is more easily to melt away[20,34-35]. Therefore, the across-model differences of sea ice extent concentration (discussed in section 3.2.2) and variability (discussed in section 3.2.3) may largely be influenced by the across-model differences of sea ice initial conditions for abrupt4xCO2.

3.2.2 Sea ice concentration

Figure 3 shows the March and September sea ice concentration

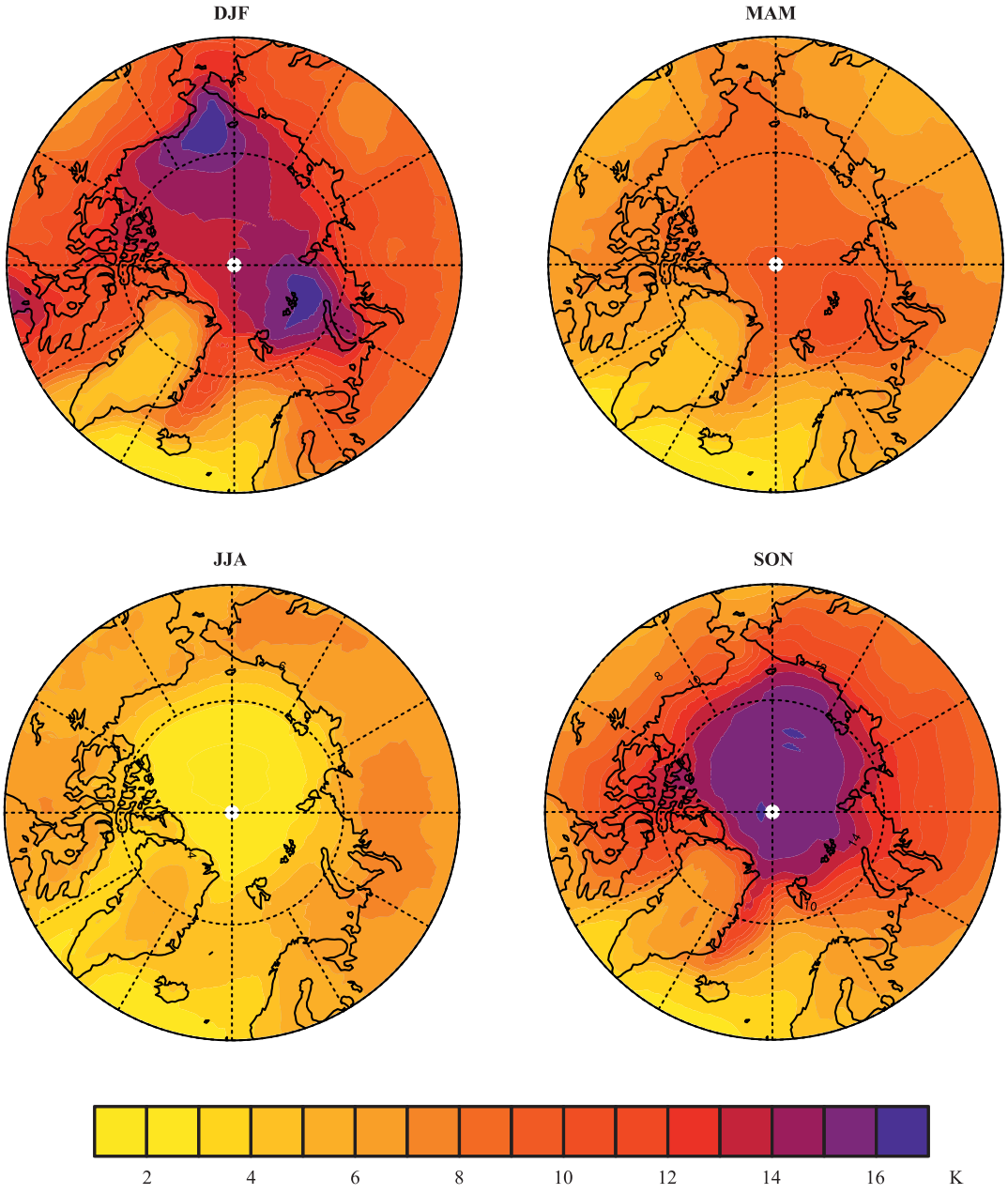

Figure 1 Multi-model ensemble mean seasonal near-surface air temperature anomalies (K) for the Arctic region for abrupt4xCO2-piControl. All models agree on the sign of change.

Table 2 Relative sea ice area change for multi-year and first-year sea ice following Zhang and Walsh[33]

Model	abrupt4xCO2		
	Relative change from piControl (%)		
	Annual	Multi-year (Sept.)	First-year (Mar.—Sept.)
BNU-ESM	–54	–93	22
CCSM4	–35	–84	57
EC-EARTH	–58	–87	19
GISS-E2-R	–29	–96	33
IPSL-CM5A-LR	–42	–81	23
MIROC-ESM	–82	–97	–37
MPI-ESM-LR	–54	–94	21
NorESM1-M	–37	–82	65
Ensemble mean	**–48**	**–89**	**25**

anomaly of abrupt4xCO2-piControl. Both sea ice concentration anomaly for multi-model ensemble mean and for each individual model (used to present the across model variation) is shown. March and September are representative of annual patterns as these two months are commonly the time when sea ice reaches its maximum and minimum extent respectively (Figure 2). The September sea ice concentration is substantially reduced by about 90% over the Arctic Ocean under abrupt4xCO2. 4 out of 8 models show zero or less than 15% sea ice concentration over the whole Arctic Ocean in September under the abrupt4xCO2 scenario (not shown). EC-EARTH simulates 15%—20% ice concentrations over the western Arctic Ocean. The other three models (CCSM4, NorESM1-M, IPSL-CM5A-LR) retain about 40% ice concentration over north of Greenland in September (not shown). The MIROC-ESM also has very low March sea ice except around the pole and in parts of the shallow seas of the Canadian Arctic Archipelago, which is attributed to its thin ice in piControl. The ensemble mean of sea ice reduction is 5% to 30% in March (Figure 3). For individual models, the largest sea ice reductions are in the Barents, Kara and Greenland seas. This can be related to the largest warming in these seas (Figure 1). Figure 3 also shows that 6 models produce sea ice increase in some regions in March: (i) The BNU-ESM shows an increase in the Greenland Sea. This is associated with changed sea ice drift along the east Greenland and westerly Jan Mayen currents that transports ice from the Greenland coast by off-coast near-surface winds[18]; (ii) CCSM4 and GISS-E2-R show an increase in the Davis Street and northern Labrador Sea. This is associated with a slight local cooling in that area in abrupt4xCO2-piControl[18].

Table 3 shows that the abrupt4xCO2 sea ice concentration changes are strongly spatially anti-correlated with temperature changes in all seasons, especially in autumn (spatial pattern correlation coefficients vary from –0.94 to –0.97) for all 8 models. This reflects the strong relation between near-surface air temperature and sea ice concentrations, such that the largely melted sea ice leads to extensive ice-free open water which inhibits rapid surface cooling in abrupt4xCO2 in autumn. In spring, all models, except MIROC-ESM, exhibit less spatial correlation between changes in surface air temperatures and sea ice concentrations under abrupt4xCO2 (Table 3, correlation coefficients from –0.53 to –0.94) compared with autumn. This suggests sea ice concentration changes during the seasons are also affected by other atmospheric and/or oceanic forcing processes, such as cyclonic activity, changed regional sea ice drift etc. These are discussed later in sections 3.3 and 3.4.

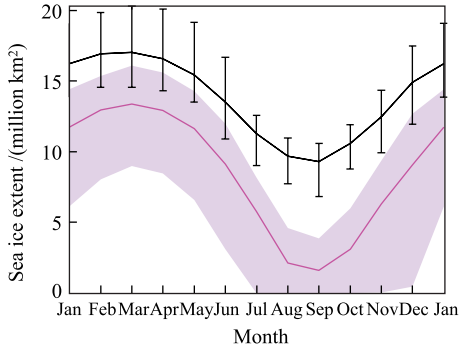

Figure 2 Multi-model ensemble mean monthly sea ice extent (following the standard definition of area of the ocean with sea ice concentration of at least 15%) for the abrupt4xCO2 (pink) and piControl (black). The ensemble mean is the thick line, the light pink band shows the full range of across-model variability (minimum to maximum) of monthly sea ice extent for abrupt4xCO2, and the error bars show the piControl across-model range.

Table 3 Pattern correlation coefficients (weighted by grid cell area) between changes of surface air temperature and sea ice concentration by season for abrupt4xCO2-piControl

ESM Model	DJF	MAM	JJA	SON
BNU-ESM	–0.72	–0.64	–0.81	–0.97
CCSM4	–0.52	–0.53	–0.78	–0.94
EC-EARTH	–0.78	–0.75	–0.76	–0.97
GISS-E2-R	–0.62	–0.60	–0.76	–0.97
IPSL-CM5A-LR	–0.72	–0.67	–0.62	–0.96
MIROC-ESM	–0.96	–0.94	–0.72	–0.94
MPI-ESM-LR	–0.76	–0.69	–0.70	–0.96
NorESM1-M	–0.60	–0.59	–0.70	–0.94
Ensemble mean	**–0.83**	**–0.80**	**–0.76**	**–0.97**

3.2.3 Sea ice cover variability

Figure 4 shows that the March and September sea ice cover interannual variability (calculated by the seasonal standard deviation of sea ice concentration to describe the year-to-year changes of the seasonal sea ice concentration) under abrupt4xCO2 is quite different than for piControl. Under piControl, the highest September sea ice cover variability

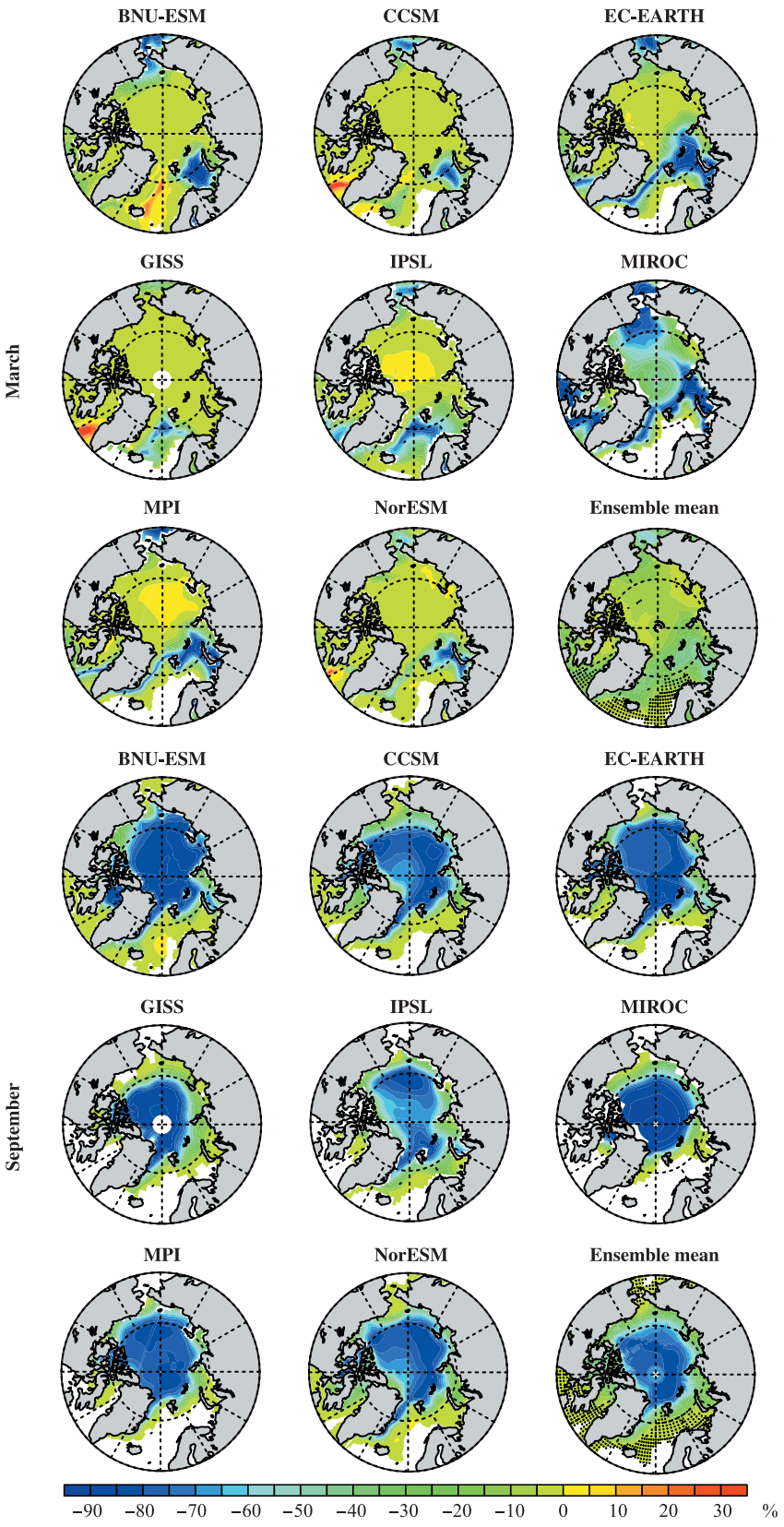

Figure 3 Model simulations of March (maximum sea ice extent) and September (minimum extent) sea ice concentration anomalies for abrupt4xCO2-piControl for the eight models we analyze here. The ensemble mean has stippling where less than six of eight models agree on the sign of change.

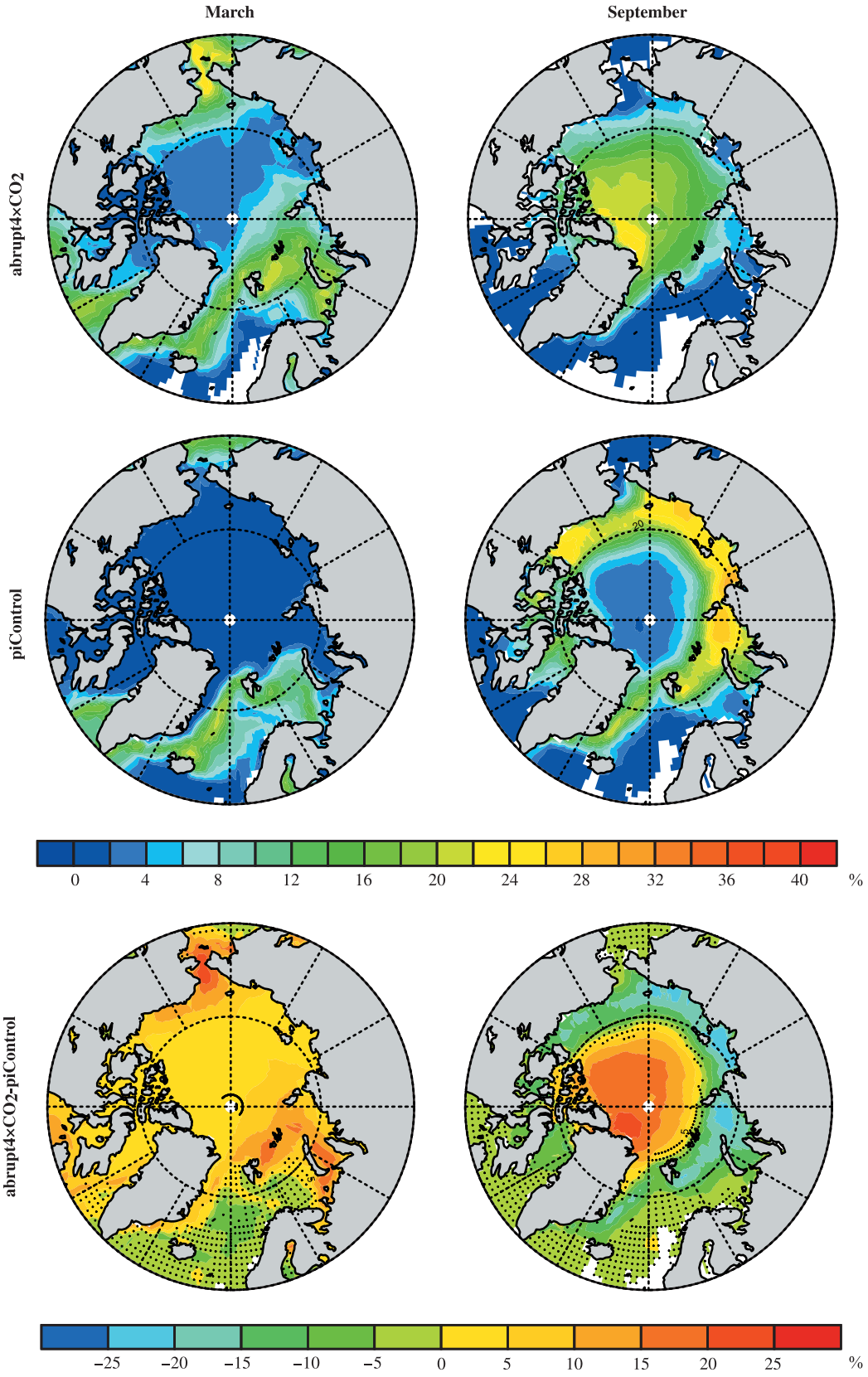

Figure 4 Simulated interannual variability of March and September sea ice concentration of ensemble means for abrupt4xCO2, piControl, and the changes abrupt4xCO2-piControl. Stippling shows where less than six of eight models agree on the sign of change.

occurs over the marginal sea ice zone close to the North American and Russian coasts, while under abrupt4xCO2, the highest September sea ice cover variability is over the area of thickest ice (north of Greenland and the Canadian Arctic Archipelago) and over the central Arctic Ocean. Under abrupt4xCO2, the March sea ice cover variability increases all over the Arctic and the September sea ice cover variability increases over the central Arctic Ocean but decreases over the marginal sea areas. These changes can be explained by the reductions in areal extent of the sea ice, with much the Arctic Ocean periphery having much lower ice concentrations in September and hence variability being lower-bound by essentially ice-free conditions. In March the increased variability reflects the increased prevalence of seasonal rather than the thicker multi-year ice cover, hence a looser, and potentially more mobile pack, if atmospheric conditions provide appropriate wind conditions.

3.3 Atmospheric circulation

Arctic surface air temperatures and sea level pressure (SLP) are linked in a suite of ocean-ice-atmosphere interactions such as synoptic-scale weather systems and cloud cover. SLP describes the near-surface atmospheric dynamics, but SLP is also coupled with atmospheric circulation at higher levels. Therefore we also examine geopotential heights at 500 hPa and the upper-tropospheric wind at 200 hPa (the height of the jet stream).

The spatial patterns of SLP anomalies (Figure 5) show some resemblance to the surface air temperature anomalies (Figure 1), especially in autumn, winter and spring: the maximum winter SLP reduction over the Barents/Kara seas and Bering/Chukchi/East Siberian seas and the maximum spring and autumn SLP reduction over the Arctic Ocean are consistent with the largest warming in these areas.

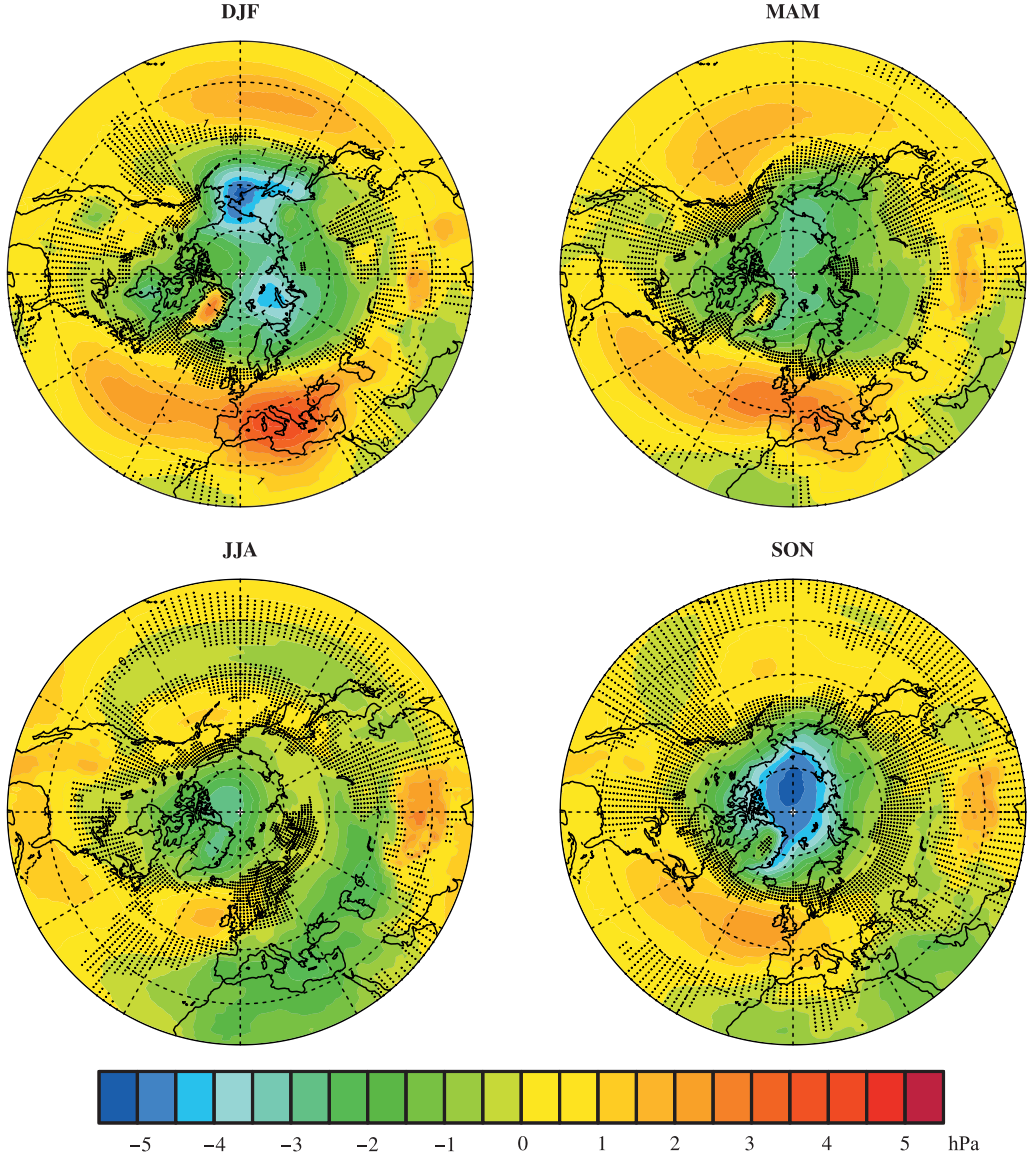

Figure 5 Multi-model ensemble mean seasonal differences of sea level pressure for the abrupt4xCO2-piControl anomalies. Stippling shows regions where less than six of eight models agree on the sign of change.

In the middle (500 hPa) troposphere, the geopotential height over whole extratropical northern hemisphere is increased in all four seasons (Figure 6). The wintertime 500 hPa geopotential height shows relatively lower increases over the North Pacific Ocean/Aleutian Low region and over Florida/southeast USA while relatively larger increases are simulated over northern Canada (Figure 6). This pattern resembles the positive phase of the Pacific North American (PNA) pattern[36] and is seen most clearly in BNU-ESM, IPSL-CM5A-LR, MPI-ESM-LR and MIROC-ESM models[18]. In summertime, the 500 hPa geopotential height shows lower increases over the Arctic Ocean and Greenland while higher increases occur over the band from 50°N—70°N (Figure 6). In general, the changes in atmospheric circulation contribute to, and feedback on, the simulated sea ice cover changes[10]. The sea ice loss modulates the near-surface conditions (albedo, surface fluxes, heat exchange between the ocean and atmosphere, etc.), which affect the atmospheric circulation due to various mechanisms (e.g. decreased static stability, increased baroclinicity and thus changed cyclone activity (section 3.4) which interact with and can change planetary waves[37].

At the 200 hPa level, the wind speed is increased most strongly in the wintertime, by 6—8 $m \cdot s^{-1}$ over central Asia, North Pacific Ocean and Gulf of Mexican (Figure 7). The wind speed increases in all seasons over the North Atlantic Ocean between eastern Canada and western Europe. The increase in 200 hPa wind is suggestive of strengthening

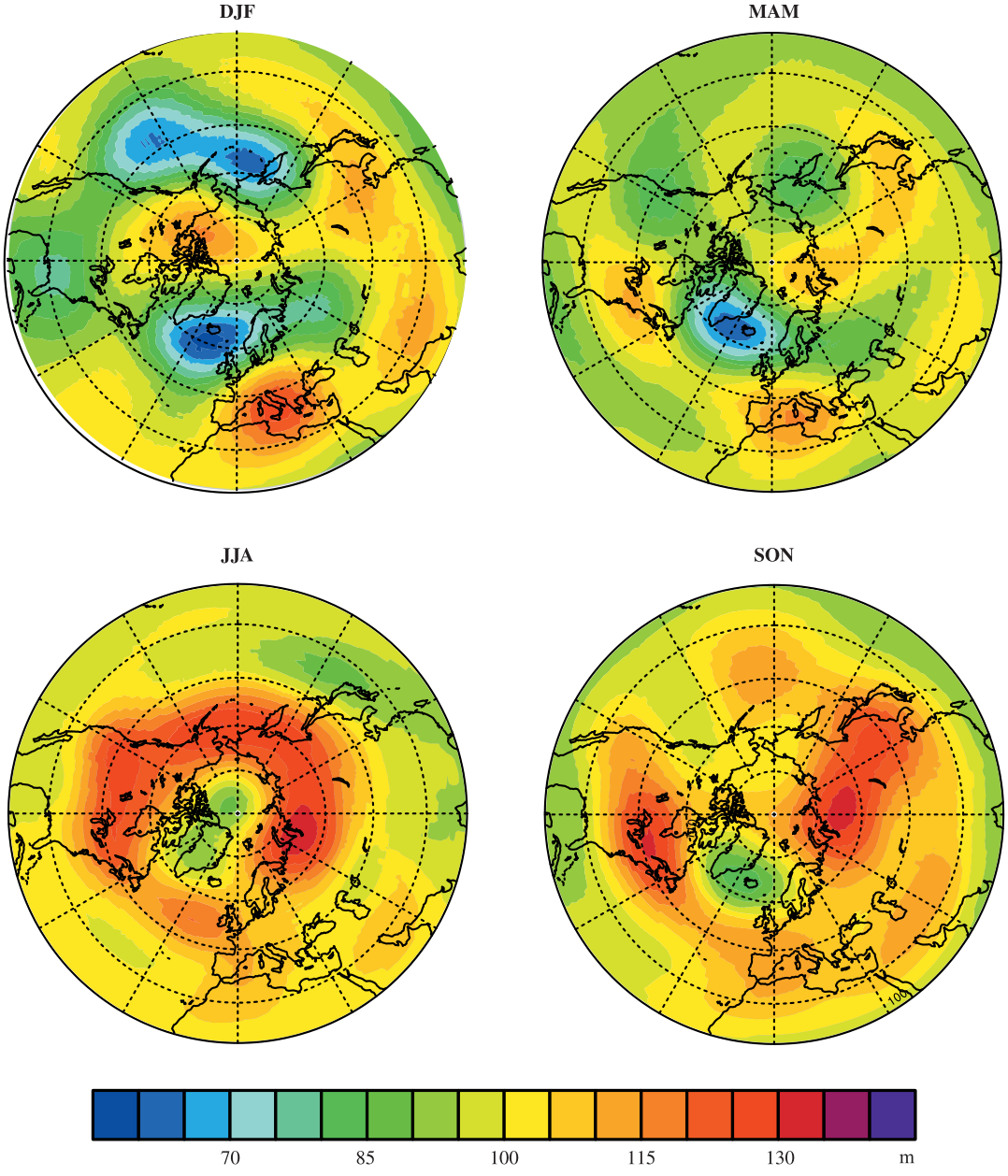

Figure 6 As for Figure 5, but for the 500 hPa geopotential height. All models agree on the sign of change.

of the upper-level jet stream. The PNA is associated with strong fluctuations in the strength and location of the East Asian jet stream[38]. The positive PNA phase implies an intensified jet stream over East Asia and the north Pacific with a slight expansion, which is demonstrated for winter in Figure 7. In our study we do not see a significant northward shift of the upper-level jets, except in autumn. Our finding of strengthened 200 hPa jet is consistent with previous climate change studies which described a strengthening, poleward shift and broadening of the upper-level jets (e.g., Lorenz and DeWeaver[39]; Collins et al.[40]) associated with the strengthening of the upper-level meridional temperature gradient. By contrast, at the 500 hPa level, the meridional temperature gradient and zonal winds are weakened due to more warming over the Arctic than elsewhere (e.g., Francis and Vavrus[41]; Vihma[10]). Increased CO_2 concentration results in tropospheric warming but a cooling in the stratosphere and raises the height of the tropopause. These temperature changes lead to an increase in the meridional temperature gradient at the upper level because the tropopause slopes downward toward the poles[39]. However, Collins et al.[40] emphasize the considerable model uncertainty in the response of the stationary waves and jets to increased greenhouse gas emissions.

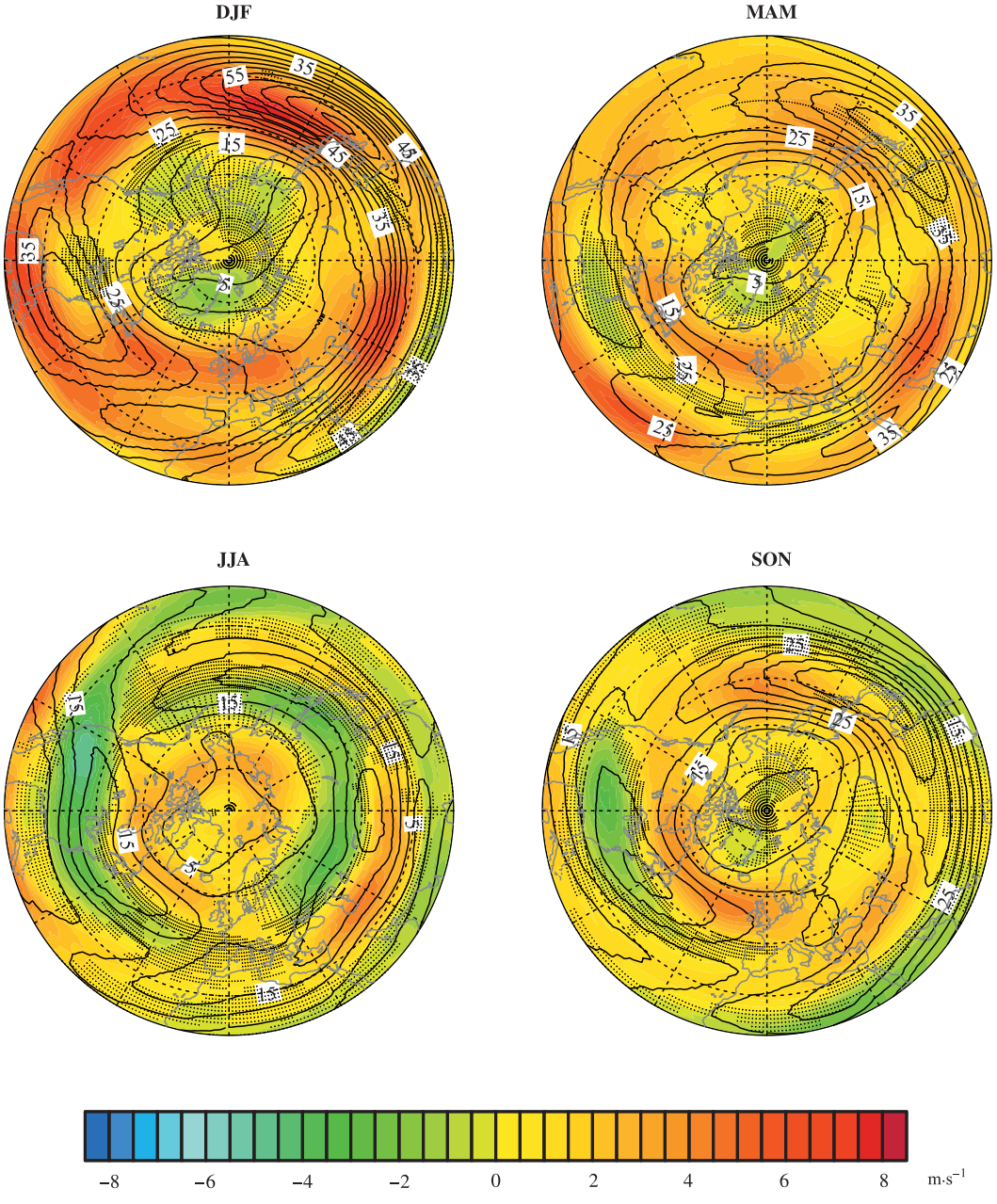

Figure 7 As for Figure 5, but for 200 hPa wind speed (color shading). Stippling shows regions where less than six of eight models agree on the sign of change. The black isolines (with intervals of 5 m·s^{-1}) show the 200 hPa wind speed in piControl.

3.4 Cyclone activity

In this study, we use the anomaly in the standard deviation of 2-6-day bandpass-filtered SLP (Figure 8) to represent changes in cyclonic activity. This method initially suggested by Blackmon[42] has been used in recent work[18, 43]. It is clear that cyclone activity is changed in all seasons under abrupt4xCO2. Figure 8 shows a significant cyclone activity increase over the northern North Atlantic, Norwegian Sea and parts of Northern Europe, and significant decrease over Canada and Alaska in winter. The cyclone activity is also significantly increased over the Arctic Ocean in summer. Cyclonic activity changes may contribute to or feedback on the sea ice changes over these regions[10]. On the one hand, cyclone activity can cause disintegration of the sea ice pack and the disintegration enhances the melting, largely due to bottom melt caused by storm-driven enhanced mixing in the ocean boundary layer[44]. Winter increase in cyclone activity in the Atlantic sector of the Arctic suggests increased penetration of cyclones bringing warmer Atlantic air (and water) much further into the Arctic enhancing the melt (or diminishing the formation) of ice. Therefore, increase in cyclone activity could cause decrease in sea ice. On the other hand, reduction of sea ice is expected to change cyclone activity by decreasing the atmospheric vertical stability and increased baroclinic instability. Consequently, the sea ice edge acts as a guide for cyclones.

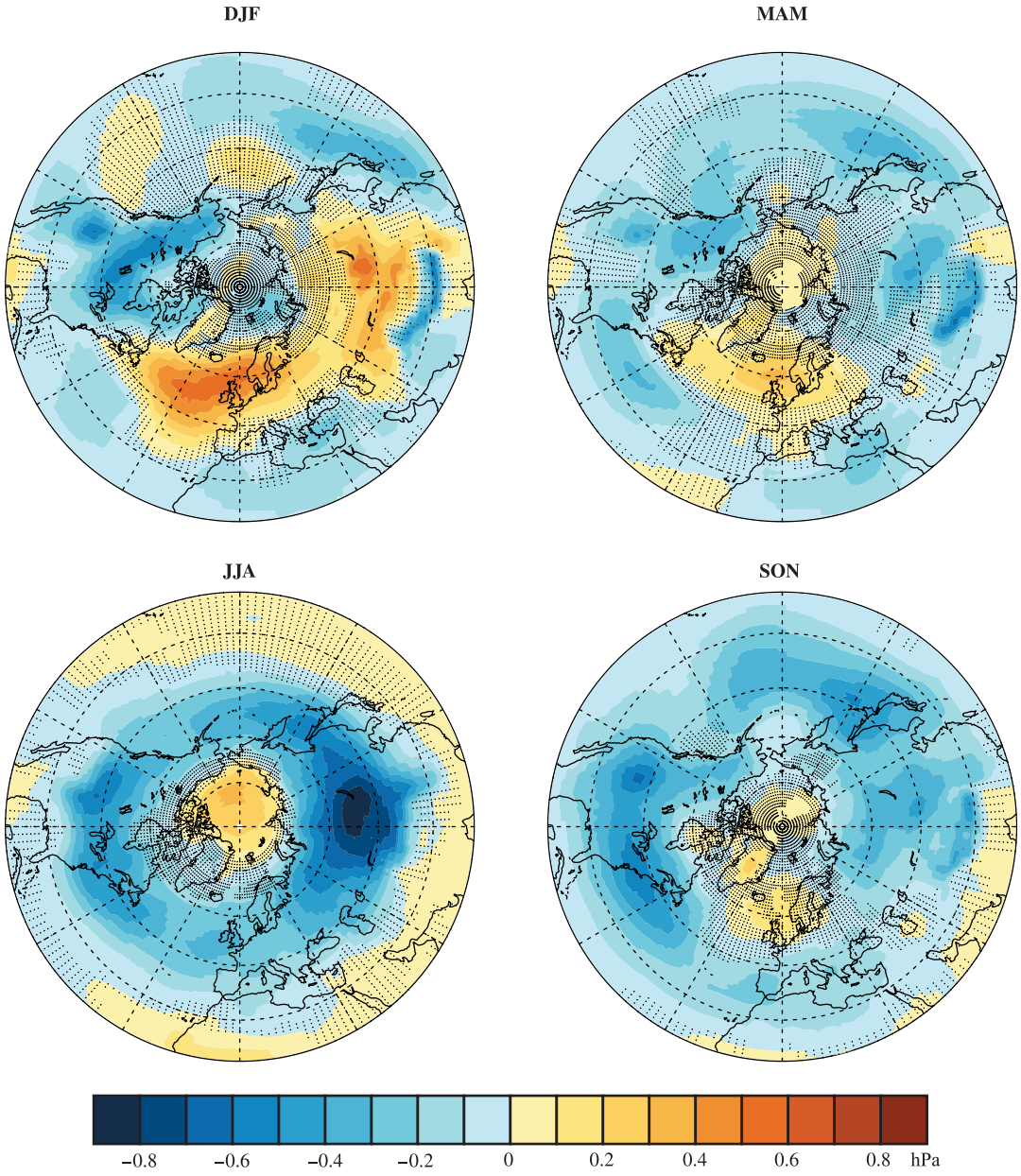

Figure 8 As for Figure 5, but for standard deviation of 2—6 d filtered sea level pressure (hPa). EC-EARTH and GISS-E2-R data were not available. The ensemble mean has stippling where less than five of six models agree on the sign of change.

4 Conclusions and implications

We describe the changes of Arctic air temperature, sea ice and atmospheric circulation under CMIP5 experiment abrupt4xCO2 relative to piControl and their impact on mid-latitude climate. Arctic sea ice decreases dramatically under abrupt4xCO2. The atmospheric circulation over the Arctic and mid-latitude region also changes, for example manifested in increased tropospheric geopotential heights and intensified upper-tropospheric jets. Arctic sea ice change is apparently strongly related to near-surface air temperature changes in all seasons, but particularly in autumn. The winter and autumn warming patterns are consistent with the regional patterns of sea ice reduction. The cyclone activity changes may contribute to or feedback on the Arctic sea ice change. However, determining the causality between them is challenging in coupled models.

Although the quadrupling of atmosphere CO_2 concentration is extreme and perhaps unrealistic, it could shed light on the possible change and impact of Arctic climate change under high levels of greenhouse gas forcing in the future. Changed jet streams and cyclone paths can bring the risk of increased winter storms to northwest Europe. However, projections of the magnitude and spatial patterns of cyclone activity changes are highly uncertain[45]. The generally good consensus on extreme winter warming, and sea ice loss between the models suggests that these changes are robust. This consensus allows us to discern fairly subtle features such as a positive phase of the PNA and also gives confidence that the simulations are at the very least plausible.

It is clear that conditions in the Arctic under quadrupled CO_2 bear little or no relation to present climate. The results would be not short of catastrophic for the ecology and human way of life in the region. Yet this is the level anticipated for greenhouse gases by the year 2100 under business as usual economic scenarios.

Acknowledgments We thank the climate modeling groups (listed in Table 1) for producing and making available their model output. We thanks the CLIVAR/WCRP Working Group on Coupled Modeling for endorsing CMIP, the scientists managing the Earth System Grid data nodes who have assisted with making CMIP output available. The U.S. Department of Energy's Program for Climate Model Diagnosis and Intercomparison provides coordinating support and led development of software infrastructure in partnership with the Global Organization for Earth System Science Portals. DJ, XY, XC and JCM thank all members of the BNU-ESM model group, as well as the Center of Information and Network Technology at Beijing Normal University for assistance in publishing the CMIP5 dataset. This work was supported by the National Basic Research Development Program of China (Grant no. 2011CB952001).

References

1 Comiso J C, Hall D K. Climate trends in the Arctic as observed from space. Wiley Interdisciplinary Reviews: Climate Change, 2014, 5: 389-409.

2 Serreze M C, Francis J A. The Arctic amplification debate. Climatic Change, 2006, 76: 241-264.

3 Walsh J E. Intensified warming of the Arctic: Causes and impacts on middle latitudes. Global and Planetary Change, 2014, 117: 52-63.

4 Meier W N, Hovelsrud G K, van Oort B E H, et al. Arctic sea ice in transformation: A review of recent observed changes and impacts on biology and human activity. Reviews of Geophysics, 2014, doi: 10.1002/2013RG000431.

5 Stroeve J C, Serreze M C, Holland M M, et al. The Arctic's rapidly shrinking sea ice cover: a research synthesis. Climatic Change, 2012, 110: 1005-1027.

6 Stroeve J C, Kattsov V, Barrett A, et al. Trends in Arctic sea ice extent from CMIP5, CMIP3 and observations. Geophysical Research Letters, 2012, 39: L16502.

7 Hezel P J, Fichefet T, Massonnet F. Modeled Arctic sea ice evolution through 2300 in CMIP5 extended RCPs. The Cryosphere Discussions, 2014, 8:1383-1406.

8 Snape T J, Forster P M. Decline of Arctic sea ice: Evaluation and weighting of CMIP5 projections. Journal of Geophysical Research: Atmospheres, 2014, 119: 546-554.

9 Deser C, Tomas R, Alexander M, et al. The seasonal atmospheric response to projected Arctic sea ice loss in the late twenty-first century. Journal of Climate, 2010, 23: 333-351.

10 Vihma T. Effects of Arctic sea ice decline on weather and climate: A review. Surveys in Geophysics, 2014. doi:10.1007/s10712-014-9284-0.

11 Chen Z, Wu R, Chen W. Impacts of autumn Arctic sea ice concentration changes on the East Asian winter monsoon variability. Journal of Climate, 2014:140415122940005.

12 Guo D, Gao Y, Bethke I, et al. Mechanism on how the spring Arctic sea ice impacts the East Asian summer monsoon. Theoretical and Applied Climatology, 2013, 115: 107-119.

13 Hilmer M, Jung T. Evidence for a recent change in the link between the North Atlantic Oscillation and Arctic sea ice export. Geophysical Research Letters, 2000, 27: 989-992.

14 Seierstad I, Bader J. Impact of a projected future Arctic sea ice reduction on extratropical storminess and the NAO. Climate Dynamics, 2009, 33: 937-943.

15 Kriegsmann A, Brümmer B. Cyclone impact on sea ice in the central Arctic Ocean: a statistical study. The Cryosphere, 2014, 8: 303-317.

16 Liu Y, Key J R. Less winter cloud aids summer 2013 Arctic sea ice return from 2012 minimum. Environmental Research Letters, 2014, 9: 044002.

17 Taylor K E, Stouffer R J, Meehl G A. An overview of CMIP5 and the experiment design. Bulletin of the American Meteorological Society, 2012, 93: 485-498.

18 Moore J C, Rinke A, Yu X Y, et al. Arctic sea ice and atmospheric circulation under the GeoMIP G1 scenario. Journal of Geophysical Research: Atmospheres, 2014, 119: 2013JD021060.

19 Kravitz B, Caldeira K, Boucher O, et al. Climate model response from the Geoengineering Model Intercomparison Project (GeoMIP). Journal of Geophysical Research: Atmospheres, 2013, 118: 8320-8332.

20 Massonnet F, Fichefet T, Goosse H, et al. Constraining projections of summer Arctic sea ice. The Cryosphere Discussions, 2012, 6: 2931-2959.

21 Curry C L, Sillmann J, Bronaugh D, et al. A multimodel examination of climate extremes in an idealized geoengineering experiment. Journal of Geophysical Research: Atmospheres, 2014, 119: 3900-3923.

22 Jones A, Haywood J M, Alterskjaer K, et al. The impact of abrupt suspension of solar radiation management (termination effect) in

experiment G2 of the Geoengineering Model Intercomparison Project (GeoMIP). Journal of Geophysical Research: Atmospheres, 2013, 118: 9743-9752.
23 Thorndike A S. A toy model linking atmospheric thermal radiation and sea ice growth. Journal of Geophysical Research: Oceans, 1992, 97: 9401-9410.
24 Bitz C M, Roe G H. A mechanism for the high rate of sea ice thinning in the Arctic Ocean. Journal of Climate, 2004, 17: 3623-3632.
25 Hunke E, Lipscomb W H. CICE: the Los Alamos 362 Sea Ice Model. Documentation and Software Users Manual, version 4.1 la-cc-06-012. New Mexico: Los Alamos National Laboratory, 2010.
26 Holland M M, Bailey D A, Briegleb B P, et al. Improved sea ice shortwave radiation physics in CCSM4: The impact of melt ponds and aerosols on Arctic sea ice. Journal of Climate, 2012, 25(5): 1413-1430.
27 Fichefet T, Maqueda M A M. Sensitivity of a global sea ice model to the treatment of ice thermodynamics and dynamics. Journal of Geophysical Research: Oceans, 1997, 102: 12609-12646.
28 Schmidt G A, Ruedy R, Hansen J E, et al. Present-day atmospheric simulations using GISS ModelE: Comparison to *in situ*, satellite, and reanalysis data. Journal of Climate, 2006, 19: 153-192.
29 Dufresne J L, Foujols M A, Denvil S, et al. Climate change projections using the IPSL-CM5 Earth System Model: from CMIP3 to CMIP5. Climate Dynamics, 2013, 40: 2123-2165.
30 K-1 Model Developers. K-1 coupled GCM (MIROC) description, K-1 Tech. Rep., 1. Tokyo: Univ. of Tokyo, 2004.
31 Notz D, Haumann F, Haak H, et al. Arctic sea-ice evolution as modeled by MPI-ESM. Journal of Advances in Modeling Earth Systems, 2013, 5: 1-22.
32 Bentsen M, Bethke I, Debernard J B, et al. The Norwegian Earth System Model, NorESM1-M – Part 1: Description and basic evaluation. Geoscientific Model Development Discussions, 2012, 5: 2843-2931.
33 Zhang X, Walsh J E. Toward a seasonally ice-covered Arctic Ocean: Scenarios from the IPCC AR4 model simulations. Journal of Climate, 2006, 19: 1730-1747.
34 Holland M M, Bitz C M. Polar amplification of climate change in coupled models. Climate Dynamics, 2003, 21: 221-232.
35 Holland M, Serreze M, Stroeve J. The sea ice mass budget of the Arctic and its future change as simulated by coupled climate models. Climate Dynamics, 2010, 34: 185-200.
36 Wallace J M, Gutzler D S. Teleconnections in the geopotential height field during the Northern Hemisphere winter. Monthly Weather Review, 1981, 109: 784-812.
37 Jaiser R, Dethloff K, Handorf D, et al. Impact of sea ice cover changes on the Northern Hemisphere atmospheric winter circulation. Tellus Series A-Dynamic Meteorology and Oceanography, 2012, 64.
38 Linkin M E, Nigam S. The North Pacific Oscillation–west pacific teleconnection pattern: Mature-phase structure and winter impacts. Journal of Climate, 2008, 21: 1979-1997.
39 Lorenz D J, DeWeaver E T. Tropopause height and zonal wind response to global warming in the IPCC scenario integrations. Journal of Geophysical Research: Atmospheres, 2007, 112: D10119.
40 Collins M, Knutti R, Arblaster J, et al. Long-term climate change: projections, commitments and irreversibility //Stocker T F, Qin D, Plattner G-K, et al. Climate change 2013: The physical science basis. Intergovernmental Panel on Climate Change, Working Group I Contribution to the IPCC Fifth Assessment Report. Cambridge, United Kingdom and New York, NY, USA: Cambridge University Press, 2013: 1071-1072
41 Francis J A, Vavrus S J. Evidence linking Arctic amplification to extreme weather in mid-latitudes. Geophysical Research Letters, 2012, 39: L06801.
42 Blackmon M L. A climatological spectral study of the 500 mb geopotential height of the Northern Hemisphere. Journal of the Atmospheric Sciences, 1976, 33: 1607-1623.
43 Woollings T, Gregory J M, Pinto J G, et al. Response of the North Atlantic storm track to climate change shaped by ocean-atmosphere coupling. Nature Geoscience, 2012, 5: 313-317.
44 Zhang J, Lindsay R, Schweiger A, et al. The impact of an intense summer cyclone on 2012 Arctic sea ice retreat. Geophysical Research Letters, 2013, 40: 720-726.
45 Eichler T P, Gaggini N, Pan Z. Impacts of global warming on Northern Hemisphere winter storm tracks in the CMIP5 model suite. Journal of Geophysical Research: Atmospheres, 2013, 118: 3919-3932.